Episodes of Strong Flow down the Western Slope of the Subtropical Andes

JOSÉ A. RUTLLANT AND RENÉ D. GARREAUD

Department of Geophysics, Universidad de Chile, Santiago, Chile

(Manuscript received 1 January 2003, in final form 5 August 2003)

ABSTRACT

Nocturnal flows down the narrow Andean valleys within the western slope of the subtropical Andes (central Chile) are episodically enhanced by easterly downslope winds that flow into the Santiago basin over the radiatively cooled air above the surface. Local, regional, and large-scale data have been used here to characterize the mean features of these episodes.

About 80% of easterly downslope flow episodes in austral winter are forced by a reversal in the sea level pressure gradient along the coast of south-central Chile, when a midlatitude cold high migrates from southern Chile eastward across the Andes under midtroposphere SW winds associated with a warm ridge aloft. Under these circumstances low-level, easterly (offshore) flow sets in, producing a compensating downslope flow that subsides over central Chile. The remaining cases are associated with prefrontal conditions under a midlatitude trough with NW winds aloft. Since in most of these cases the easterly low-level flow occurs beneath westerly flow higher above, these episodes classify as strong windward downslope flows.

Within the Andean valleys and canyons, the near-surface air experiences a sensible warming and drying at night and early morning during these episodes, as the strong downvalley winds tend to destroy the surface-based radiative inversion and mix down warmer air from aloft. At the exit region of these valleys into the central basin, these downslope flows in austral winter are not able to flush the cold air pool there. Hence, dawn surface temperatures over the basin tend to be lower than average as clear skies and dry subsiding air aloft favor surface radiative cooling. The resulting enhancement of the near-surface static stability hampers the subsequent development of the mixed layer, leading to severe air pollution events in Santiago and other cities in central Chile. A comparative discussion on governing mechanisms with respect to apparently similar phenomena, as gap flow and shallow foehn, is included.

1. Introduction

The subtropical west coast of South America is under the influence of the southeast Pacific anticyclone throughout the year, resulting in a semiarid climate with almost all precipitation (300–400 mm per year) concentrated in the austral winter (June–August) and a very stable lower troposphere. Between 33° and 35°S (central Chile), the region's topography is characterized by three main units (Fig. 1). Moving east of the Pacific seashore there is a coastal range that in many places rises above 1500-m elevation, a central depression with its floor at 500–600 m above sea level (ASL), and the Andes Cordillera, which rises sharply to an average elevation of 4000 m ASL, with some summits above 6000 m, no passes below 3000 m, and a half-width of about 100 km. Three major rivers cross this region with an average east–west direction, forming narrow valleys in the Andes range and widening westward over the central depression. Of particular interest, the Santiago basin within the central depression is crossed by the Maipo River and is confined to the north and south by two secondary transversal ranges (Fig. 1).

Strong flows down the western slope of the subtropical Andes occur several times per month, mostly at nighttime and early morning, gusting up to 20 m s^{-1} at the exit regions of the Andean valleys into the central depression. While these easterly flows seldom reach damaging speeds, they do have a significant impact in the regional weather. Proceeding from north to south, local names such as *Terral*, *Raco*, and *Puelche* are common for these winds in the regional weather lore. They bring unusually dry and warm spells, especially in austral winter. The spreading of the warm air on top of the denser, radiatively cooled air over the low lands of the central depression often results in the strengthening and sinking of the mean subsidence inversion. In particular, *Raco* winds flowing from the Maipo River Canyon lead to air pollution episodes in Santiago, the Chilean capital, currently with more than five million inhabitants (e.g., Rutllant and Garreaud 1995; Gallardo et al. 2002).

Episodes of strong downslope flow are observed in many other mountain ranges around the world, their interpretation/analysis/forecasting is still a hot topic in

Corresponding author address: René Garreaud, Department of Geophysics, Universidad de Chile, Blanco Encalada 2085, Santiago, Chile.
E-mail: rgarreau@dgf.uchile.cl

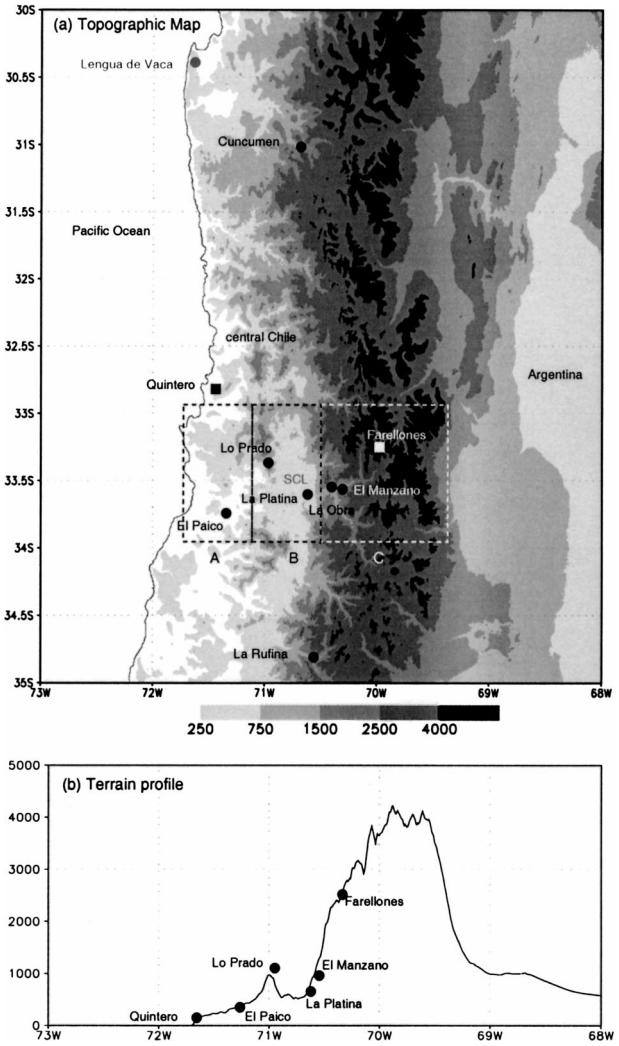

FIG. 1. (a) Topographic map of central Chile. Shading scale in m ASL. The thin line is the Pacific coast. Location of surface (upper air) stations are indicated by filled circles (squares). SCL indicates approximate location of the Santiago downtown. The boxes labeled C, B, and A indicate the Andes Cordillera, the central depression, and the coastal range, respectively. (b) Cross-range terrain profile averaged between 33° and 34°S.

mountain meteorology (e.g., Colle and Mass 1998; Nance and Colman 2000). The usual large-scale setup for such mesoscale phenomena includes a cross-barrier flow over a ridge, whereupon strong flows down the lee slope may develop. The most intense episodes, referred to as downslope windstorms, derive from a mountain lee-wave amplification and subsequent breaking, bringing cross-mountain momentum down to the surface [for a review of mechanisms see Durran (1990)]. The amplification results from the reflection of the upward-propagating gravity waves due to the presence of an inversion or stable layer near crest level (Klemp and Lilly 1975) and/or the presence of levels of 0 ambient wind or flow reversal (the so-called critical levels; e.g., Klemp and Lilly 1978) above crest level. The critical level may even arise from the breaking of a growing gravity wave (Peltier and Clark 1979). Alternatively, Durran (1986) proposed a hydraulic framework in which strong downslope winds are associated with a transition from subcritical to supercritical ambient flow at crest level and a subsequent ''hydraulic jump'' effect down the lee slope. Mountain wave amplification and hydraulic dynamics have been applied to diagnose windstorms along the lee slopes of the Rockies (e.g., Klemp and Durran 1987), southeast Alaska (Colman and Dierking 1992), the Cascades (e.g., Colle and Mass 1998), the Dinaric Alps (Smith 1987), and the east side of the subtropical Andes (Seluchi et al. 2003).

Here we focus on the characterization of the mean regional and synoptic-scale circulation patterns during the occurrence of strong downslope wind events over the westward side of the Andes in central Chile. To this end, we have selected a number of episodes and documented their mean features by means of a compositing analysis of key surface, upper-air, and reanalysis data. Though we focus here on the upper Maipo River valley, as it exits into the Santiago basin and has more available data, we also document the regional manifestation of these events to the north and south of this area (see Fig. 1).

The paper is organized as follows: Section 2 describes the available meteorological data (local, regional, and large-scale) relevant to the characterization of this phenomenon. The longer-term series are also used to describe some features of the regional background flow in section 3. Section 4 describes the episode selection and basic statistics. Composite large-scale patterns and regional features are documented in sections 5 and 6, respectively. A discussion of possible forcing mechanisms and a comparison with downslope wind events in other mountain ranges are presented in section 7. Finally, a summary of our main findings is presented in section 8.

2. Datasets

Primary surface data include hourly observations from three automatic weather stations within the Maipo River valley: El Manzano, La Obra, and El Paico (see Fig. 1 and Table 1 for details). Data are, in general, available from 1997 to 2001, with a shorter period at La Obra. El Manzano and La Obra are located in the upper Maipo River valley, to the east of the Santiago central basin. El Paico is located about 60 km from the seashore in the lower, wider portion of the valley. Two additional nearby stations have been considered: La Platina, within the Santiago basin close to the Andes foothills, and Lo Prado, on a saddle point of the coastal range at about 1000 m ASL and 30 km west of downtown Santiago. Complementing this local network, two automatic weather stations were installed during 2001 at Cuncumen (upper Choapa valley; 31°S) and La Rufina (upper Tinguiririca valley; 34.7°S), about 200 km to the

TABLE 1. Surface stations. Variables measured are pressure (p), air temperature (T), relative humidity (RH), and wind and speed direction (**u**). Upper-air (radiosonde/pibal) stations are also indicated.

Station	Latitude (S)	Longitude (W)	Elevation (m ASL)	Variables	Period
Cuncumen	31°54′	70°37′	1120	*T*, RH, **u**	2001
Quintero	32°47′	71°32′	8	Radiosonde	1997–2001
Farellones	33°21′	70°18′	2300	Pibal	1997
Lo Prado	33°27′	70°56′	1065	*T*, RH, **u**	1997–2001
La Obra	33°36′	70°29′	720	*T*, RH, **u,** Pibal	2001
El Manzano	33°35′	70°22′	875	*T*, RH, **u**	1997–2001
La Platina	33°34′	70°32′	620	Wind profiler	1998–2001
El Paico	33°42′	71°00′	255	*p*	1997–2000
La Rufina	34°45′	70°45′	820	*T*, RH, **u**	2001

north and south of the Maipo valley, respectively. Upper-air data from the Quintero (33.2°S, 71.5°W; 7 m ASL; at the coast about 100 km WNW of Santiago) radiosonde station, and from a 915-MHz wind profiler equipped with a radio acoustic sounding system (RASS) at La Platina were also considered. Several 1-day field campaigns near La Obra consisting of 30-g pilot-balloon observations with optical theodolite at 0800, 1100, and 1400 LT [local time (LT) = UTC − 0400] were performed when suitable conditions occurred during the austral winter of 2001. Large-scale circulation patterns were characterized using National Centers for Environmental Prediction–National Center for Atmospheric Research (NCEP–NCAR) reanalysis fields, described in detail in Kalnay et al. (1996). Here we have used mandatory pressure-level fields, with 12-h resolution on a 2.5° × 2.5° latitude–longitude grid (about 280-km grid spacing at these latitudes).

3. Background flow

At the coastal radiosonde station of Quintero, average winds in the free atmosphere near the top of the Andes (5 km) present a year-round dominance of the WNW direction (Rutllant 1983a). Below that level the northerly wind component strengthens in response to the mechanical blocking of the flow by the Andes. Previous observations in the same area (Rutllant 1983a,b; Kalthoff et al. 2002) show that close to the mountains these NW winds may often present a jetlike structure (''barrier jet'') that results from the damming of a statically stable incoming westerly flow against the Andes and the subsequent slope overpressure and geostrophic adjustment (e.g., Schwerdtfeger 1975; Parish 1982). Given the average height ($H \sim$ 4000–4500 m ASL) and half-width ($L \sim$ 100 km) of the subtropical Andes, and typical values for midtropospheric zonal flow ($U \sim 10$ m s^{-1}) and static stability ($N \sim 1.2$–1.5×10^{-2} s^{-1}), the Froude number is much smaller than unity (0.1–0.2), resulting in an effective blocking of the westerly flow within a Rossby radius of deformation of about 500 km.

The mean vertical structure of the diurnal cycle of the regional circulation close to the Andes foothills in the austral winter is illustrated in Fig. 2 from the wind profiler at La Platina (reliable data only cover the first 1300 m AGL, i.e., 1900 m ASL). Above 900 m AGL (~1500 m ASL) enhanced northerlies, nearly uniform throughout the day, result from the aforementioned blocking effect of the Andes. Below this level there is a marked diurnal cycle in the zonal flow, likely associated with a mountain–valley breeze system favored by a large diurnal cycle of the sensible heat flux over the bare slopes (e.g., Whiteman 1990). Easterly flow reaches its maximum strength around 600 m AGL at nighttime and early morning, being prevented from penetrating below by the radiation temperature inversion over the Santiago basin. Later in the morning the upslope flow develops, peaking in intensity with a SW direction in the late afternoon at about 250 m AGL, following the development of the daytime surface mixed layer over the basin (Ulriksen 1980). The summertime mean circulation is similar to the one depicted in Fig. 2, but with a stronger and deeper SW flow during the afternoon (not shown).

Figure 3 illustrates the characteristic diurnal/seasonal cycles of the near-surface wind (1997–99) at El Manzano, La Platina, and Lo Prado. At all these stations a wind reversal from light easterly wind components at night and early morning to stronger westerlies in the afternoon is evident. The latter are particularly strong during the high-sun season. Because of local orographic influences, zonal wind components become enhanced at El Manzano and Lo Prado, although easterlies peak at different seasons. At El Manzano enhanced easterlies in winter are likely associated with a stronger downvalley drainage flow.

4. Episode selection and basic statistics

The frequency distributions of early morning (0600–0800 LT) along-valley wind speeds at El Manzano and La Obra are shown in Fig. 4, in which a bimodal condition is evident, with a gap around −3.5 m s^{-1} (negative values indicate downvalley flow). The lower speed mode of the distribution corresponds to local downvalley flow; the higher speed mode is what we refer to as strong regional-scale downslope flow. Strong downslope flow days at El Manzano (*Raco* days) were defined as days in which the hourly averaged downvalley wind speeds exceeded a threshold of

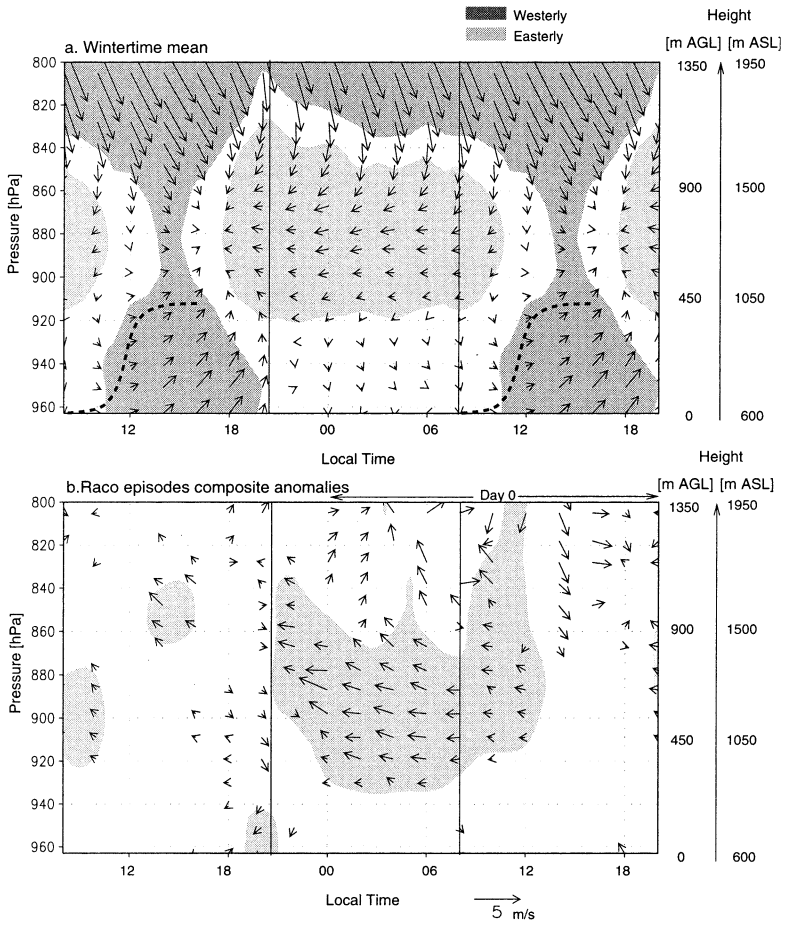

FIG. 2. (a) Austral winter mean diurnal cycle of the wind (arrows) and zonal wind (shaded) obtained from the wind-profiler hourly observations at La Platina (SE Santiago). Wind direction is shown in the conventional form: an arrow pointing downward indicates northerly wind, an arrow pointing to the left indicates easterly flow, etc. Wind speed is scaled according to the arrow length shown at the bottom. Westerly winds in excess of 1 m s^{-1} are shown in dark shading. Easterly winds in excess of 0.5 m s^{-1} are shown in light shading. Vertical solid lines indicate approximately sunset and sunrise times. Dashed lines indicate wintertime average height of the mixed layer over Santiago. (b) Composite anomalies of the wind (arrows) during *Raco* episodes. Only wind vectors statistically significant at the 95% confidence level are shown. Light shading indicates easterly wind anomalies in excess of 1.5 m s^{-1}.

-5 m s^{-1} between 0400 and 0700 LT.[1] This threshold roughly corresponds to the lower decile in the total upvalley wind speed distribution during austral winter, filtering out weaker summertime episodes. The higher occurrence of Raco days in wintertime is consistent not only with the stronger seasonal average of the downvalley wind speeds at El Manzano (Fig. 3a), but also with the stronger synoptic-scale forcing over central Chile during that season.

Forty-six Raco episodes, defined as those with one or more consecutive Raco days, were selected in the winter months of 1997, 1998, 1999, and 2001. Raco episodes were typically 1–2 days in duration, only ~20% of them lasting 3–4 days. The average return period of Raco episodes is about one per week, reflecting the typical time frame of midlatitude synoptic wave patterns, though the variability is large (standard deviation of 2.7 days). Scatterplots of 0400–0700 LT along-valley wind speeds at El Manzano/Cuncumen and El Manzano/La Rufina are presented in Figs. 5a,b. Although speeds were on average stronger at El Manzano, the correspondence of strong downvalley winds (lower decile of the individual distributions) is fairly good, illustrating the regional nature of Raco events in central Chile. In summary, we are selecting Raco events responding to a strong regional forcing over which the local, light wind regime is superimposed.

[1] Hourly average wind speeds of 5 m s^{-1} are likely associated with wind gusts in excess of 10 m s^{-1} (e.g., Brasseur 2001).

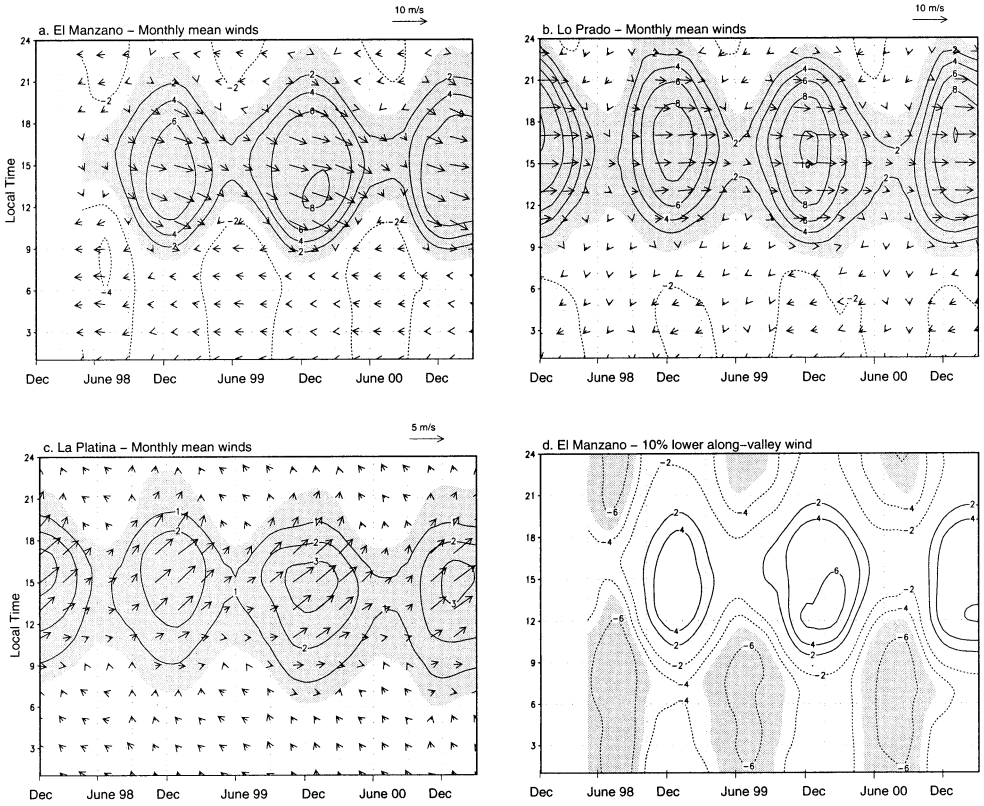

FIG. 3. Monthly mean diurnal and annual cycles of the wind (arrows) at (a) El Manzano, (b) Lo Prado, and (c) La Platina. Wind direction is shown in the conventional format. Wind speed is scaled according to the scale at the top of each panel (note different scale for La Platina). Zonal wind is contoured every 2 m s^{-1} in El Manzano and Lo Prado and every 1 m s^{-1} in La Platina. The 0 contour is omitted, and negative values are in dashed lines. Westerly flow is indicated by light shading. (d) Along-valley wind speed corresponding to the lower 10% of the monthly distribution at each hour at El Manzano. Contour interval is 2 m s^{-1}; the 0 contour has been omitted, and negative values (downvalley) are in dashed lines. Values less than -5 m s^{-1} are shown in light shading.

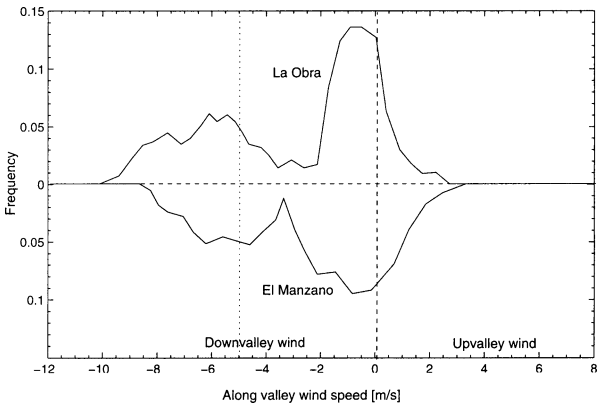

FIG. 4. Frequency distribution of early morning (0600–0800 LT) along-valley wind speeds at La Obra and El Manzano (fliped down for sake of clarity) during austral winter (May–Aug: 2000–01 for La Obra; 1998–2001 for El Manzano). Negative values indicate downvalley flow.

5. Synoptic weather patterns

From the pool of Raco episodes selected during the austral winters of 1997–2001, dates corresponding to 1-day episodes and to the peak of longer episodes (hereafter referred to as ''day 0'') were analyzed. A visual screening of the weather maps for each day 0 reveals that nearly 80% of the cases are associated with postfrontal conditions in central Chile (group A) and the remaining 20% are associated with prefrontal conditions (group B). There are a number of common features within the members of each group, synthesized in Fig. 6 by the group-average (composite) maps of sea level pressure (SLP) and 500-hPa geopotential height at 1200 UTC (0800 LT) for day 0 that we describe below. The dynamical forcing is discussed later in section 7.

In group A, the 500-hPa circulation is characterized by a ridge–trough pattern over southern South America, with the ridge axis to the west of the Andes at the time of the strongest downvalley winds in central Chile (Fig. 6a). Therefore, southwesterlies prevail over the subtropical Andes (5000 m ASL) during most Raco days.

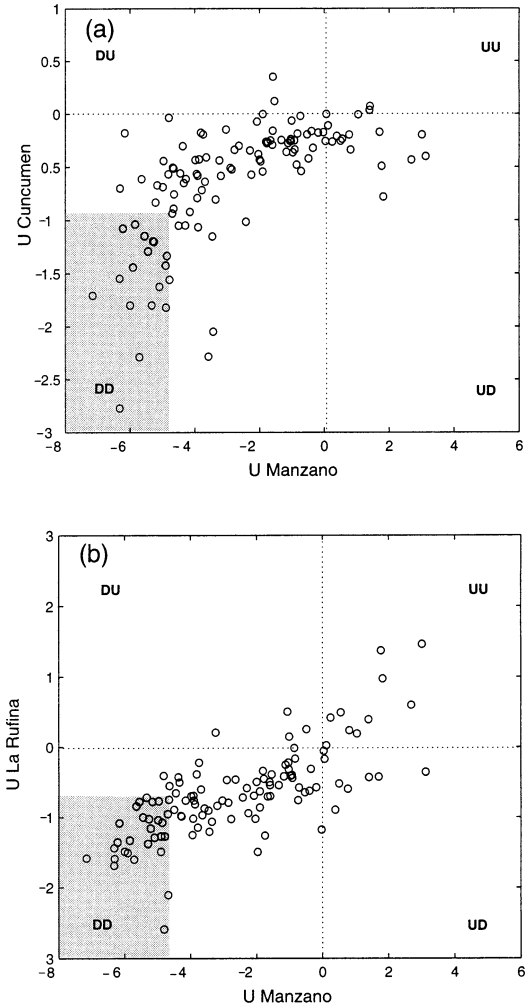

FIG. 5. Scatterplot of the along-valley wind speed averaged between 0400–0700 LT at (a) El Manzano/Cuncumen and (b) El Manzano/La Rufina. Negative values indicate downvalley flow. Shaded areas are bounded by the lower 10% of the individual frequency distributions.

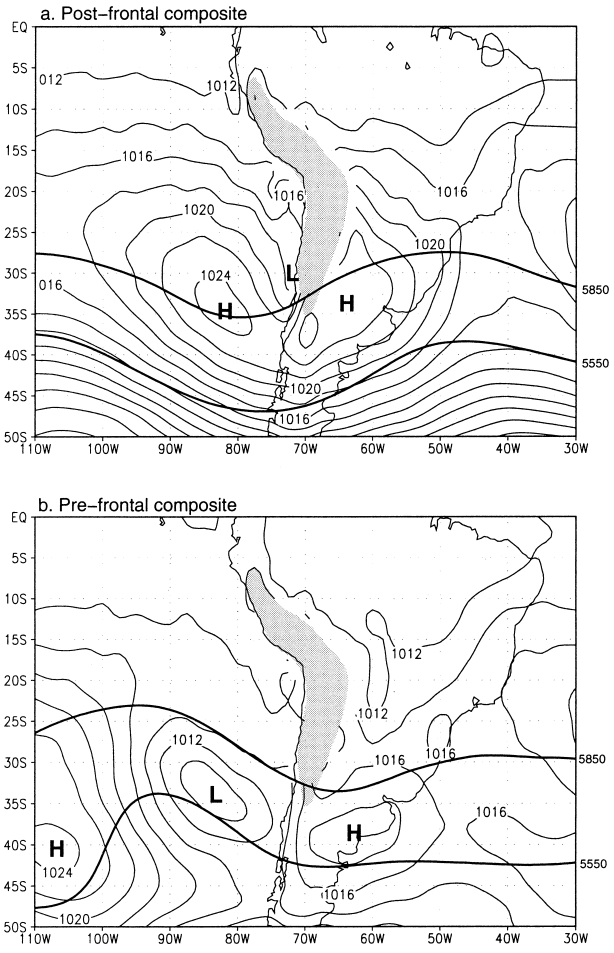

FIG. 6. Composite weather maps for (a) postfrontal (group A) and (b) prefrontal (group B) strong downslope wind days at 1200 UTC (0800 LT). SLP is contoured every 2 hPa. Shown in thick lines are 500-hPa geopotential height contours of 5850 and 5550 gpm. Gray areas indicate terrain elevation in excess of 3000 m ASL.

Inspection of composite winds at other levels shows that westerly flow over central Chile extends from upper levels down to ~700 hPa. At the surface, a migratory cold anticyclone with its center tracking at about 40°S protrudes over Argentina to the east of the subtropical Andes behind a cold front that has reached the South Atlantic by this time. Even at this coarse resolution, a narrow trough along the coast of Chile is evident. This recurrent pattern of high–low–high surface pressure across the subtropical Andes is described in detail in Garreaud et al. (2002) and Garreaud and Rutllant (2003), as it is associated with the development of coastal lows (or coastal troughs) in central Chile and cold surges to the east of the subtropical Andes.

The remaining 20% of Raco episodes (group B) are associated with a midlatitude depression drifting abnormally north of the climatological storm track over the SE Pacific (40°–50°S). Raco episodes in the Andean valleys occur then as prefrontal conditions when the midlatitude low is just off south-central Chile (Fig. 6b). In the midtroposphere, the phase of the midlatitude wave has reversed with respect to group A, with a trough axis just to the west of the Andes over central Chile. In any case, Raco episodes within group B are associated with strong northwesterly flow aloft.

6. Regional features

Time sequences of several surface and upper-air observations below the crest of the Andes were centered on day 0 (the peak of each Raco episode at El Manzano) and averaged to produce composite time series. Twenty-four 1-day, postfrontal Raco episodes (group A) were considered in this analysis. Composite anomalies were defined at each hour as the difference between the composite and the long-term seasonal average. The statistical significance of the hourly composite anomalies was

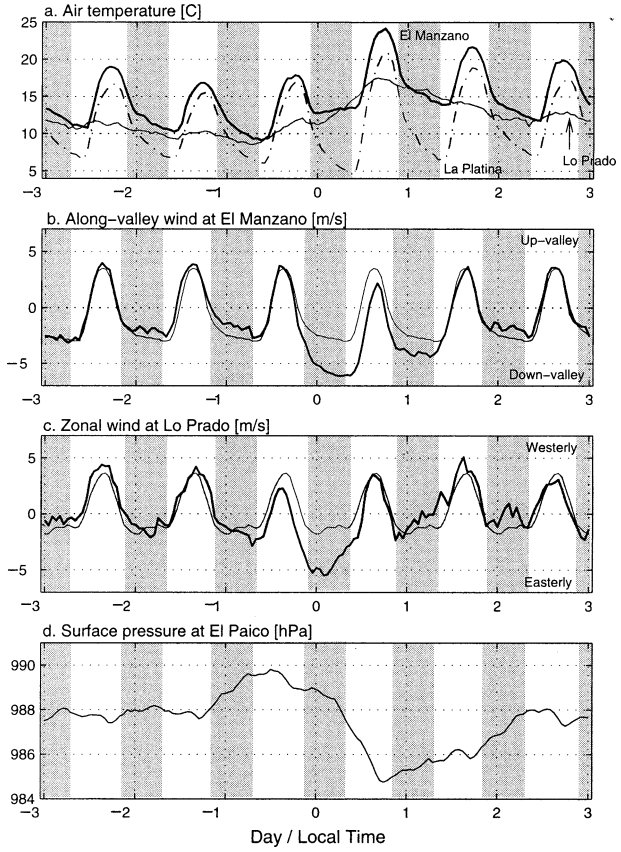

FIG. 7. Composite time series of several near-surface variables centered on day 0 [peak of each strong downslope wind (Raco) episode at El Manzano]. Light shaded areas indicate nighttime periods. (a) Air temperature at El Manzano (thick solid line), La Platina (dot–dashed line), and Lo Prado (thin solid line). (b) Along-valley wind speed composite at El Manzano (thick line) and seasonal mean (thin line). Negative values indicate downvalley flow. (c) Zonal wind composite at La Obra (thick line) and seasonal mean (thin line). (d) Surface pressure at El Paico.

tested locally using a two-tailed Student's *t* test at the 95% confidence level.

a. Andean valleys

Consistent with the episode's selection, the composite along-valley wind at El Manzano exhibits a downvalley wind anomaly throughout day 0, although statistical significance is reached only during dawn and early morning (Fig. 7b), when the downvalley wind speed is at least twice as strong as the seasonal average. This conspicuous diurnal cycle of the wind anomaly along the valley axis is evident in nearly all individual Raco episodes, regardless of their duration. At the exit region of the Maipo valley into the Santiago central basin (La Obra), the early morning easterly flow exhibits a jetlike structure in which maximum speeds reach typical values of 10 m s^{-1} within the first 100–300 m above the surface, as revealed by individual wind profiles during four Raco episodes (Fig. 8). The maximum downvalley speed near the surface is independent of the magnitude (and even the sign) of the zonal flow aloft. This easterly jet loses strength toward noon, associated with the onset of upvalley flow in a shallow surface layer below the jet. Composite downvalley wind anomalies in the other two instrumented Andean valleys (Cuncumen and La Rufina stations) tend to begin simultaneously with those at El Manzano (not shown). Inspection of individual cases, however, reveals a large dispersion in the initial time among the stations (standard deviation of 4 h), although it always occurs after the evening of day −1.

At El Manzano, nighttime air temperatures during the Raco episodes are much warmer than the seasonal mean, as the strong downvalley winds tend to destroy the surface-based radiative inversion by mixing down warmer air from aloft (Fig. 7a). Such nocturnal and early morning warming is one of the most sensible effects of the Raco episodes in the Maipo Canyon, also evident in other Andean valleys of central Chile (not shown). Warmer morning temperatures, clear skies, and enhanced subsidence explain the warm anomalies in the afternoon of day 0: about 8°C in the composite and as large as 15°C in individual *Raco* episodes.

b. Central depression and beyond

Insights into the vertical structure of the easterly flow downstream from the Andes foothills can be obtained from the composite time–height wind anomalies at La Platina (Fig. 2b). Easterly wind anomalies aloft during the night and early morning of day 0 attain maximum speeds between 200 and 400 m above the central depression, consistent with the composite wind anomalies observed at Lo Prado (Fig. 7c). The composite zonal winds at Lo Prado and El Manzano are broadly similar, but significant anomalies at Lo Prado lead those at El Manzano by ~18 h. The detachment of the strong easterly flow from the nocturnal surface inversion over the central valley is also evident, consistent with the absence of significant surface wind anomalies at La Platina. Recall that the central depression is bounded to the west by a well-developed coastal range with its crest level at about 1000 m ASL (~500 m above the central depression's ground level).

To further illustrate the westward extension of the easterly flow during Raco days, vertical wind profiles in a near-zonal cross section at 33°S from Quintero (seashore) to Farellones (Andes slope; 2300 m ASL and 30 km east of Santiago) for 15 April 1980 at 0800 LT (Rutllant and Saavedra 1983) are presented in Fig. 9 for both zonal and meridional wind components. On that occasion a coastal low culminated (minimum SLP) over the area on the morning of 16 April. Along this westward cross-range section the layer of easterly flow extended from the surface to about 2000 m ASL, widening downstream. It is also worthwhile noting the geographical confinement of the NNW barrier jet, conspicuously absent at Quintero (about 100 km west of Santiago),

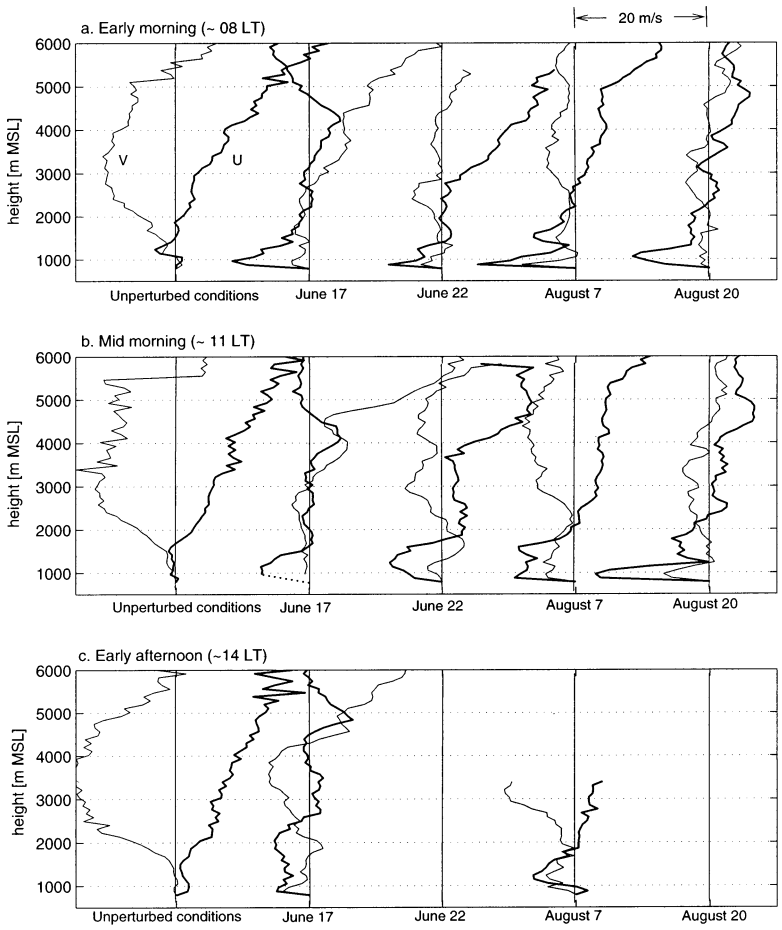

FIG. 8. Vertical profiles of the zonal (*U*; thick lines) and meridional wind (*V*; thin lines) components measured at La Obra (exit region of the Maipo Canyon) at (a) 0800, (b) 1100, and (c) 1400 LT. Speed scale is above (a). Included in (a)–(c) are 5 columns: the leftmost column corresponds to the average of 5 days not classified as strong downslope flow days (unperturbed condition). The rest of the columns correspond to 4 strong downslope days during the austral winter of 2001 (dates indicated at the bottom).

where only light northerlies appear between 2500 and 3500 m ASL. The southerly component of the wind above 3500-m elevation is consistent with the position of the warm ridge axis aloft.

The air temperature at Lo Prado exhibits a very small diurnal cycle (Fig. 7a), consistent with its location atop a 35-m telecommunications tower, with a very good correspondence with the free atmosphere (Quintero) temperature at the 900-hPa level (Rutllant and Garreaud 1995). At this station, a gradual warming (and drying; not shown) begins in the early morning of day -1, at the time of the onset of the easterly anomalies there, and continues until midafternoon of day 0. At the end of most Raco episodes, there is an abrupt cooling associated with an energetic recovery of the marine boundary layer and associated westerly onshore advection of colder air, as the regional enhanced subsidence/easterly flow ceases to act. Note that the composite analysis shows only a gradual cooling after day 0 because the compositing technique smears out this feature.

The surface air over the Santiago basin (represented by La Platina) remains within the cold-air pool during the night and early morning, leading to low minimum air temperatures on day 0, as the clear skies and the dry subsiding air favor the surface radiative cooling, in sharp contrast with the warm air temperature over the Andean valleys. The pronounced temperature gradient between the cold air near the surface and the warmer air aloft during early morning hampers the subsequent development of the surface mixed layer during daytime, leading to severe air pollution episodes in Santiago (e.g., Rutllant and Garreaud 1995). This also results in high afternoon maximum temperatures and a large amplitude of the diurnal cycle (Fig. 7a).

Consistent with the synoptic-scale pattern depicted by the reanalysis data, the composite surface pressure

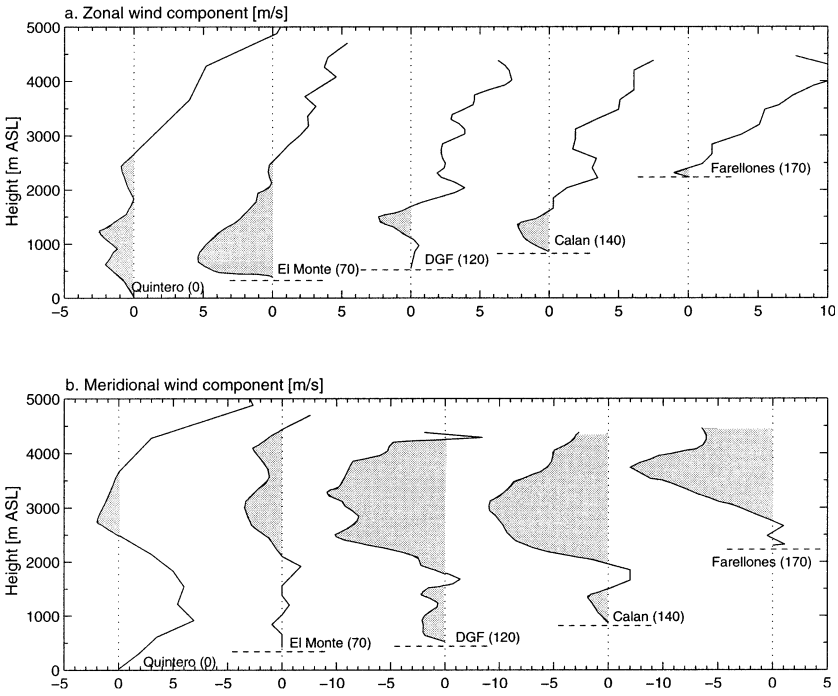

FIG. 9. Vertical profiles of the (a) zonal and (b) meridional wind components measured at five stations within the Maipo basin on 15 Apr 1980 at 0800 LT. On that day, a coastal low culminated in central Chile, a condition typically associated with strong flow down the western slope of the Andes. The stations' names and distances to the coastline are indicated at the bottom of each profile. Dashed lines indicate the ground level of each station. In (a) and (b), shaded areas indicate easterly and northerly flow, respectively.

at El Paico (Fig. 7d) exhibits an increase in surface pressure during the night and early morning of day −1, associated with the strengthening of the subtropical anticyclone by colder air behind a frontal disturbance that just passed over south-central Chile. During the second half of day −1 the surface pressure begins to drop, almost simultaneously with the onset of the easterly flow anomalies at Lo Prado (Fig. 7c), down to a minimum by late afternoon of day 0, signaling the culmination of the coastal low (or trough) in central Chile. Later, the onset of the westerly anomalies at Lo Prado coincides with the rise in the surface pressure at El Paico on day +1.

7. Discussion

Strong downvalley flows tend to occur simultaneously within the Andean valleys in central Chile and extend westward over the central depression and coastal range, even past the seashore. What is the dynamical forcing of such regional scale low-level easterly flow? In the first place, we note that easterly Raco events in both groups A and B occur mostly under a westerly flow component at mid- and upper levels (e.g., Fig. 8). The transition between easterly and westerly flow (critical level) over central Chile is typically found at ~700 hPa, well below the Andes crest level (~500 hPa). The phenomenon described here could therefore be termed as *windward* strong downslope flow, in contrast to the most common *lee* slope cases (as briefly reviewed in our introduction). Alternatively, Raco events could be classified as ''shallow foehn'' (e.g., Sprenger and Schär 2001). Let us first explore the mechanism behind the most common postfrontal Raco events (group A).

The surface map depicted in Fig. 6a shows a well-defined cross-range pressure gradient at the latitudes of interest that arises from the presence of a warm-core coastal trough (or low) to the west of the Andes and a cold-core high to the east of the range. Similar cross-range gradients are found to be instrumental for windstorms along the western side of the Washington Cascade Mountains (e.g., Colle and Mass 1998). Nevertheless, the mean altitude of the Andes (~5000 m ASL) and the high altitude of the few gaps (mountain passes above 3500 m ASL) preclude any possible gap flow driven by this surface pressure gradient. To further substantiate this idea with actual observations, Fig. 10a illustrates cross-range horizontal differences in pressure and air temperature at different heights between Mendoza (Argentina) and Quintero (Chile) for 17 group A Raco days in austral winter 1998. Bands encompassing values within ±one standard deviation of the corresponding mean differences indicate that a west–east cross-range pressure gradient only exists below 3000 m

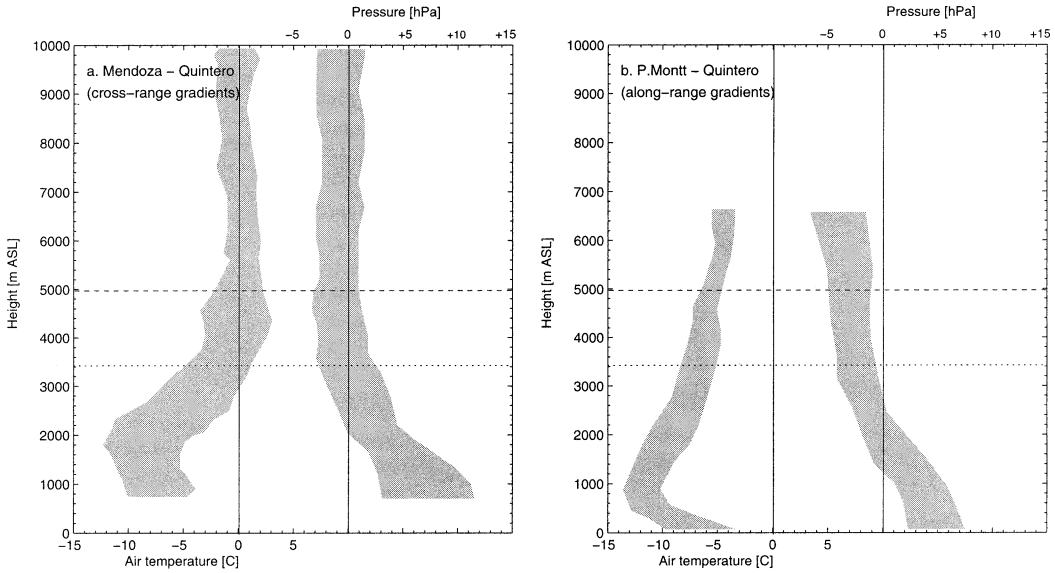

FIG. 10. (a) Pressure and temperature differences between Mendoza (32.5°S, 68.5°W, 830 m ASL; east of the Andes) and Quintero (32.8°S, 71.3°W, 8 m ASL; west of the Andes) for 17 Raco cases in austral winter 1998. Bands correspond to 1 std dev above and below the corresponding mean difference. Pressure (temperature) difference corresponds to the right (left) band, with its scale on top (bottom) of the graph. (b) As in (a), but for differences between Puerto Montt (41.2°S, 72.5°W, 86 m ASL; southern Chile) and Quintero (central Chile). Dashed and dotted horizontal lines indicate mean Andean crest level and lowest Andean gaps, respectively.

ASL and that above 3500 m this gradient changes sign consistent with the position of the ridge axis to the west of the Andes.

The surface map (Fig. 6a) also shows a poleward pressure gradient along the coast of south-central Chile during Raco events, primarily caused by the passage of a cold-core anticyclone in southern Chile. The corresponding along-range differences in pressure–temperature between Puerto Montt (41.5°S) and Quintero (33°S) for 17 Raco days (Fig. 10b) lend support to the reanalysis-based composite and show maximum pressure differences within the first 1000 m ASL. Offshore easterlies develop in (geostrophic) response to such a meridional low-level pressure gradient force, as shown numerically by Garreaud and Rutllant (2003). This offshore flow forces subsidence over the western slope of the Andes through mass continuity requirements ($w \simeq u\partial h_m/\partial x$, where h_m is the mountain height), which enhances the large-scale subsidence ahead of the midlevel ridge axis. It is suggested then that strong downvalley flow within the zonally oriented Andean valleys is triggered and sustained by the regional-scale easterly flow, being modified by local orographic effects. Furthermore, enhanced subsidence west of the Andes within a very stable environment leads to mid- and low-level warming and the corresponding coastal troughing. This latter effect implies a positive feedback on the easterly offshore flow as the north–south SLP gradient strengthens (Garreaud and Rutllant 2003).

Given the westerly flow at crest level, wave amplification or hydraulic jump analogs are thus of little help to explain easterly Raco events, except for the relatively few cases (one out of five cases within group A) in which the midtroposphere wave pattern amplifies with a NW–SE tilt in the ridge axis, eventually leading to a cutoff low off northern Chile. In these cases, there are SSE winds on top of the Andes whereupon a classical foehn-like pattern develops. Nevertheless, this subset of cases does not present speeds significantly different from the rest of group A.

At this point, beyond the simple 2D scheme across a knife-edge, meridionally oriented Andes, along-range flow components come into consideration. In group A, a midtroposphere (approximately Andes crest level) ridge axis located just west of the Andes results in southwesterly winds. Following Sprenger and Schär (2001), an along-range flow could result in a shallow flow (shallow foehn) toward large-scale lower pressures within a cross-range gap, since winds become subgeostrophic. In the case discussed here, such a flow would produce a westerly (upslope) component over the Andean valleys, that is, opposite to the observed easterly (downslope) flow. Within Group B, opposite midtroposphere synoptic conditions prevail, with the trough axis just west of the Andes. Here an easterly gap flow component could help in the maintenance of the easterly downslope flow that arises from the convergence into the frontal trough, as suggested in Rutllant and Garreaud (1995). It has to be said here that since group B synoptic conditions result from the evolution of those characterizing group A as a full midtropospheric wave crosses the Andes, mixed transition conditions can be expected in the case of fast-moving waves. Numerical simulations (e.g., Zängl 2002) would be therefore required to assess

the relative importance of 3D flow on the resulting strong downslope winds, including time-dependent transition from group A to B.

One interesting regional aspect of the Raco events is that the strongest/significant easterly (downvalley) wind anomalies are restricted to nighttime and early morning. Such a marked diurnal cycle of the along-valley surface wind anomalies during Raco events is not expected from the random timing of the dynamic forcing of these events. Nevertheless, the warm ridge aloft during most Raco events is typically associated with clear skies that favor the daytime surface heating of the sloping terrain and, hence, stronger than average upslope flows.

8. Conclusions

The average regional circulation over central Chile results from the perturbation that the large-scale westerly flow experiences as it encounters the massive subtropical Andes through mechanical and thermal effects. The regional circulation can be divided into a surface boundary layer about 2 km deep controlled by the thermal contrast between the Andes western slope and the free atmosphere to the west, resulting in a diurnal oscillation of the low-level, cross-range flow. A second layer up to the Andes summit (~5 km) feels the mechanical blocking of the Andes to the westerly flow (small Froude number) with barrier-jet-like northerlies along the slope. A low-level, slope-induced thermal low pressure through solar heating at daytime is compatible with a high-level, slope-induced high pressure caused by the damming of the impinging large-scale flow aloft.

About 80% of the Raco events occur as a warm ridge at midlevel is just to the west of the subtropical Andes. Under these circumstances, the typical equatorward pressure gradient along the coast of south-central Chile is reversed by a cold anticyclone crossing the Andes in southern Chile. In geostrophic response to such a meridional pressure gradient, regional-scale, low-level easterly (offshore) flow develops at the coast and inland, triggering and sustaining most of the strong downslope wind events within the Andean valleys. Since only one out of five of these events experiences easterly flow components atop of the Andes (lee downslope flow), the phenomenon described in this study generally corresponds to *windward* downslope flow or a shallow foehn. The remaining 20% of Raco events are associated with a surface midlatitude low near the west coast of central Chile and a midtroposphere (crest level) cold trough.

Strong downslope wind events are associated with a general warming of the lower troposphere over central Chile, mostly due to the vertical advection of warm air (Garreaud and Rutllant 2003). Within the Andean valleys, the near-surface air temperature experiences a very sensible warming (and drying) during the night and early morning of these days, as the strong downvalley winds tend to destroy the surface-based radiative inversion by mixing down warmer (and dryer) air from aloft. These downslope flows are, however, not able to flush the cold-air pool over the central depression. Hence, surface dawn temperatures there tend to be lower than average as the clear skies and dry subsiding air favor the surface radiative cooling. The resulting enhanced static stability hampers the subsequent development of the mixed layer and leads to severe air pollution events in Santiago and other cities along the central depression. Consequently, the major effect of these windward strong downslope flows is not to produce hazardous weather at the exit region of the Andean valleys into the central depression, but instead a condition prone to severe air pollution episodes in Santiago, one of the most heavily polluted cities in South America.

Acknowledgments. This research was supported by FONDECYT (Chile) under Grant 1000913. Meteorological data from La Platina, El Manzano, Lo Prado, and El Paico were kindly provided by Centro Nacional del Medio Ambiente (CENMA), Universidad de Chile; special thanks are due to P. Ulriksen, A. Cabello, and M. Araya. Radiosonde data from Quintero were kindly provided by Direccion Meteorologica de Chile. NCEP–NCAR reanalysis data were obtained from NOAA's Climate Diagnostics Center. We also wish to thank the collaboration of several people during the field work of this project, especially Mrs. Patricia Angoy, director of Colegio Almenar del Maipo, and her colleagues, the Director and Prof. Sergio Salinas of Escuela Publica Cuncumen and Mr. Ramon Esposito from Junta de Vigilancia Rio Maipo. We also thank Prof. Roberto Roman and Mr. Ricardo Bustos for their valuable support throughout this project. Special thanks are due to Dr. T. Parish and two anonymous reviewers who helped to significantly improve this manuscript.

REFERENCES

Brasseur, O., 2001: Development and application of a physical approach to estimating wind gusts. *Mon. Wea. Rev.,* **129,** 5–25.

Colle, B. A., and C. F. Mass, 1998: Windstorms along the western side of the Washington Cascade Mountains. Part I: A high-resolution observational and modeling study of the 12 February 1995 event. *Mon. Wea. Rev.,* **126,** 28–52.

Colman, B. R., and C. F. Dierking, 1992: The Taku wind off southeast Alaska: Its identification and prediction. *Wea. Forecasting,* **7,** 49–64.

Durran, D. R., 1986: Another look at downslope windstorms. Part I: On the development of supercritical flow in an infinitely deep, continuously stratified fluid. *J. Atmos. Sci.,* **43,** 2527–2543.

——, 1990: Mountain waves and downslope winds. *Atmospheric Processes over Complex Terrain, Meteor. Monogr.,* No. 45, Amer. Meteor. Soc., 59–81.

Gallardo, L., G. Olivares, J. Langner, and B. Aarhus, 2002: Coastal lows and sulfur air pollution in Central Chile. *Atmos. Environ.,* **36,** 315–330.

Garreaud, R. D., and J. Rutllant, 2003: Coastal lows along the subtropical west coast of South America: Numerical simulation of a typical case. *Mon. Wea. Rev.,* **131,** 891–908.

——, ——, and H. Fuenzalida, 2002: Coastal lows along the sub-

tropical west coast of South America: Mean structure and evolution. *Mon. Wea. Rev.,* **130,** 75–88.
Kalnay, E., and Coauthors, 1996: The NCEP/NCAR 40-Year Reanalysis Project. *Bull. Amer. Meteor. Soc.,* **77,** 437–471.
Kalthoff, N., and Coauthors, 2002: Mesoscale wind regimes in Chile at 30°S. *J. Appl. Meteor.,* **41,** 953–970.
Klemp, J. B., and D. K. Lilly, 1975: The dynamics of wave-induced downslope winds. *J. Atmos. Sci.,* **32,** 320–339.
——, and ——, 1978: Numerical simulation of hydrostatic mountain waves. *J. Atmos. Sci.,* **35,** 78–107.
——, and D. R. Durran, 1987: Numerical modeling of bora winds. *Meteor. Atmos. Phys.,* **36,** 215–227.
Nance, L., and B. Colman, 2000: Evaluating the use of a nonlinear two-dimensional model in downslope wind forecasting. *Wea. Forecasting,* **15,** 715–729.
Parish, T., 1982: Barrier winds along the Sierra Nevada mountains. *J. Appl. Meteor.,* **21,** 925–930.
Peltier, W. R., and T. L. Clark, 1979: The evolution and stability of finite-amplitude mountain waves. Part II: Surface wave drag and severe downslope windstorms. *J. Atmos. Sci.,* **36,** 1498–1529.
Rutllant, J., 1983a: Vientos de barrera en los Andes de Chile Central (Barrier winds in the Andes of central Chile). *Frontera,* **1,** 49–52. [Special issue in Spanish, available from R. Garreaud.]
——, 1983b: Coastal lows in central Chile. Preprints, *First Int. Conf. on Southern Hemisphere Meteorology,* Sao Jose dos Campos, Brazil, Amer. Meteor. Soc., 334–346.
——, and N. Saavedra, 1983: Un perfil aerológico transversal sobre Chile central: Campaña Farellones 1980. Project Report, 62 pp. [Available from R. Garreaud.]
——, and R. Garreaud, 1995: Meteorological air pollution potential for Santiago, Chile: Towards an objective episode forecasting. *Environ. Monit. Assess.,* **34** (3), 223–244.
Schwerdtfeger, W., 1975: The effect of the Antarctic Peninsula on the temperature regime of the Wedell Sea. *Mon. Wea. Rev.,* **103,** 45–51.
Seluchi, M., F. Norte, P. Satyamurty, and S. Chan-Chou, 2003: Analysis of three situations of the foehn effect over the Andes (Zonda Wind) using the Eta–CPTEC Regional Model. *Wea. Forecasting,* **18,** 481–501.
Smith, R. B., 1987: Aerial observations of the Yugoslavian Bora. *J. Atmos. Sci.,* **44,** 269–297.
Sprenger, M., and C. Schär, 2001: Rotational aspects of stratified gap flows and shallow föhn. *Quart. J. Roy. Meteor. Soc.,* **127,** 161–187.
Ulriksen, P., 1980: Diurnal variations of the mixed layer over Santiago (in Spanish). *Tralka,* **1** (2), 143–151. [Available from R. Garreaud.]
Whiteman, C. D., 1990: Observations of thermally developed wind systems in mountainous terrain. *Atmospheric Processes over Complex Terrain, Meteor. Monogr.,* No. 45, Amer. Meteor. Soc., 5–42.
Zängl, G., 2002: Stratified flow over a mountain with a gap: Linear theory and numerical simulations. *Quart. J. Roy. Meteor. Soc.,* **128,** 927–949.